



Instrumentation and Sensors – Acoustics

Paul Geimer, Andrew Delorey
Los Alamos National Laboratory

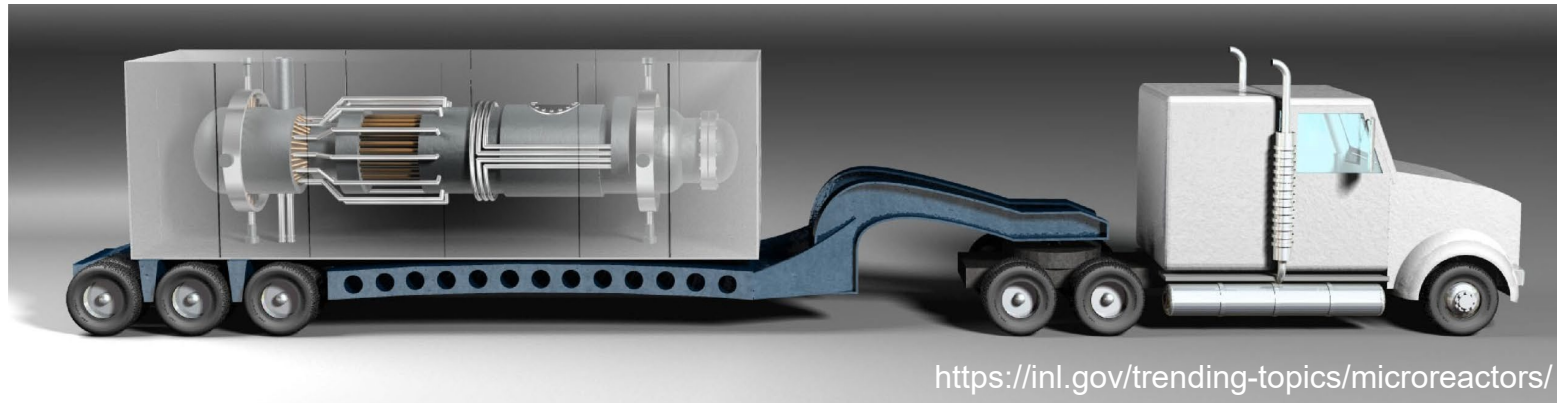
March 4, 2026

Microreactor Program Annual Winter Review

Motivation: Advancing structural health monitoring readiness for microreactor applications

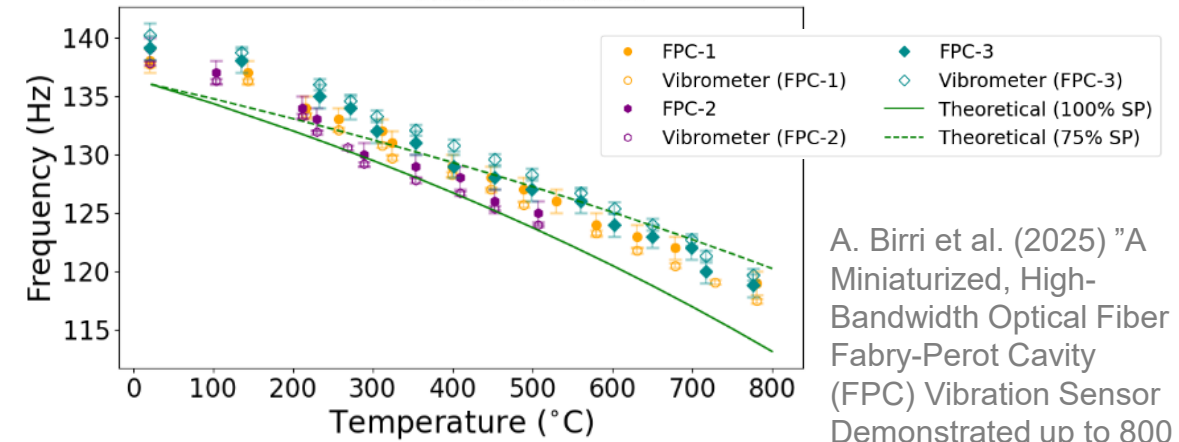
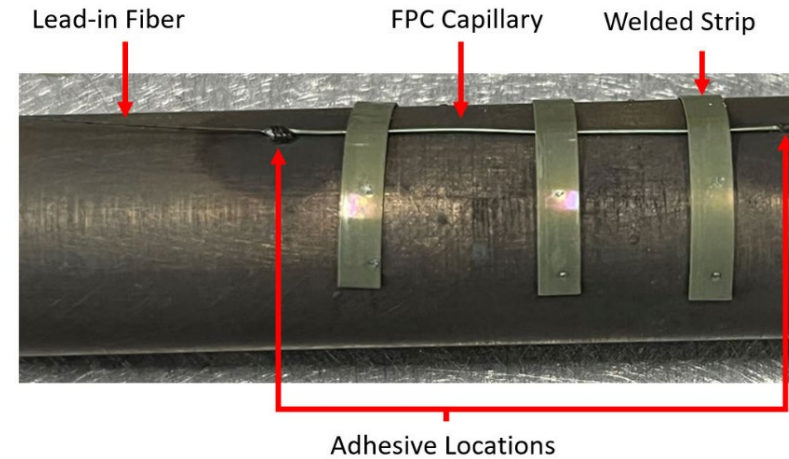
Goal: Enable condition-based monitoring to reduce technical and operational risks

- Improve operational autonomy in remote environments
- Reduce inspection burden
- Support qualification for long-duration deployments



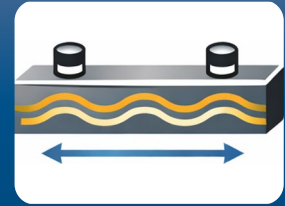
Structural anomaly characterization using in-situ vibration / acoustic measurements

- If fiber-based sensors can measure high-bandwidth vibrations in high-temperature environments, how to best utilize similar signals for in-situ structural health monitoring?
- How well can localized anomaly detection be achieved in both one and two dimensions?



A. Birri et al. (2025) "A Miniaturized, High-Bandwidth Optical Fiber Fabry-Perot Cavity (FPC) Vibration Sensor Demonstrated up to 800 °C" *IEEE Sens. J.*

Acoustic techniques for structural health monitoring



Guided waves



Impulse / ringdown



Acoustic emissions

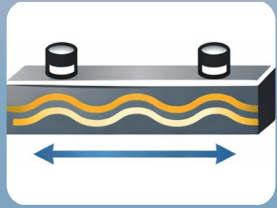


Modal analysis

Active

Passive

Acoustic techniques for structural health monitoring



Guided waves



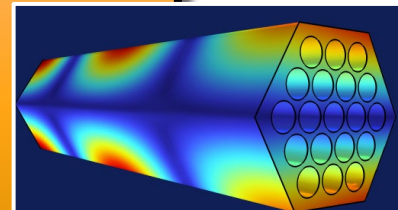
Impulse / ringdown



Acoustic emissions

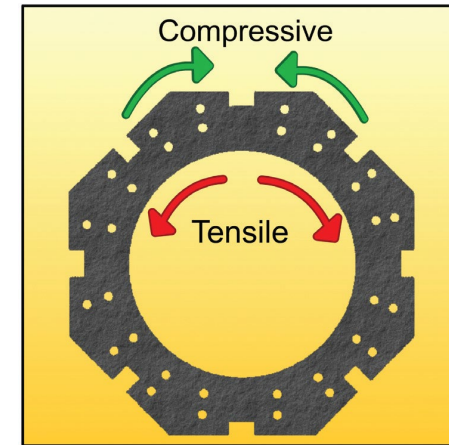


Modal analysis

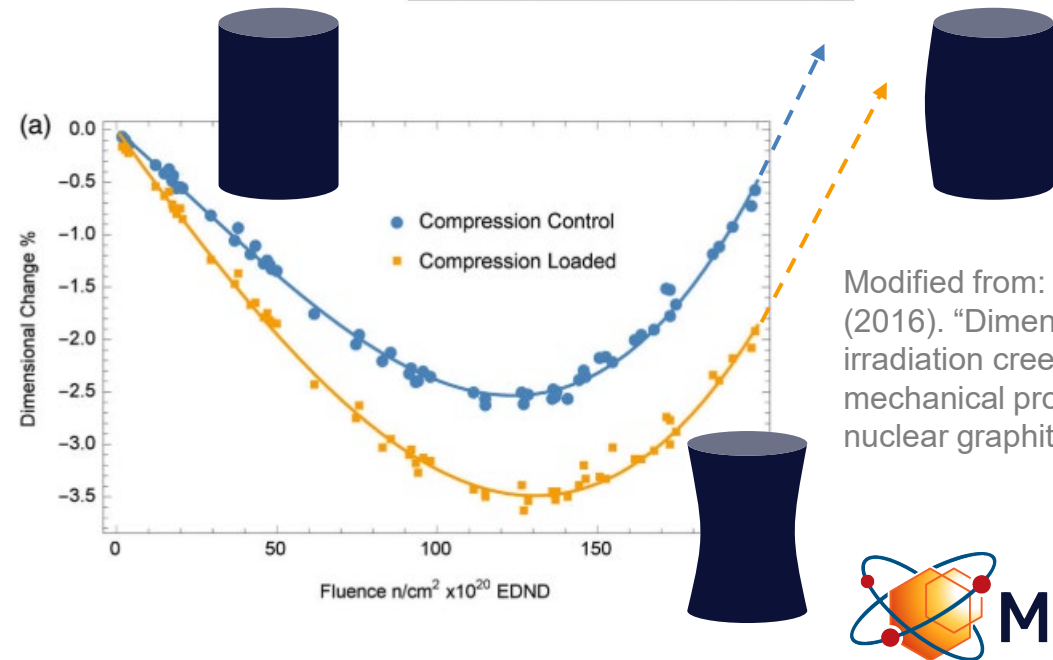


FY25/26 efforts have focused on graphite components

- Graphite fracture toughness is $\sim 50\text{-}100\times$ less than stainless steel
- Creep, dimensional change, thermal expansion are all affected by fluence
 - Transition from shrinkage to swelling (“turnaround”) shifts to lower fluence as irradiation temperatures increase
- Hunterston B shutdown moved up by 2+ years after inspection discovered 100s of cracks in graphite core bricks

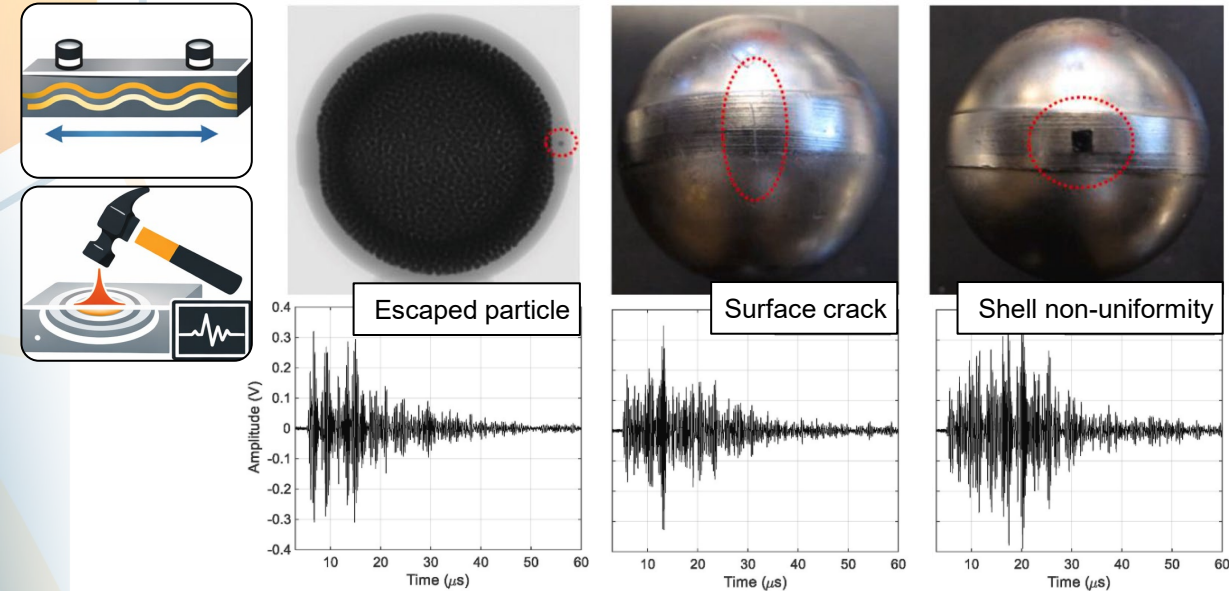


Maul et al. (2017).
“Cracking in Nuclear Graphite”
Math. Today.



Modified from: Marsden et al. (2016). “Dimensional change, irradiation creep and thermal / mechanical property changes in nuclear graphite” *Int. Mat. Rev.*

Incorporating deep learning into graphite inspection

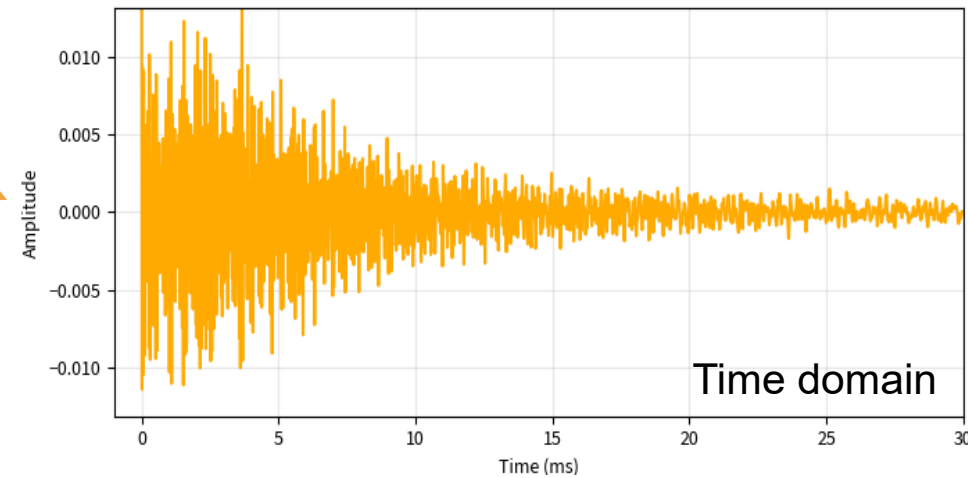
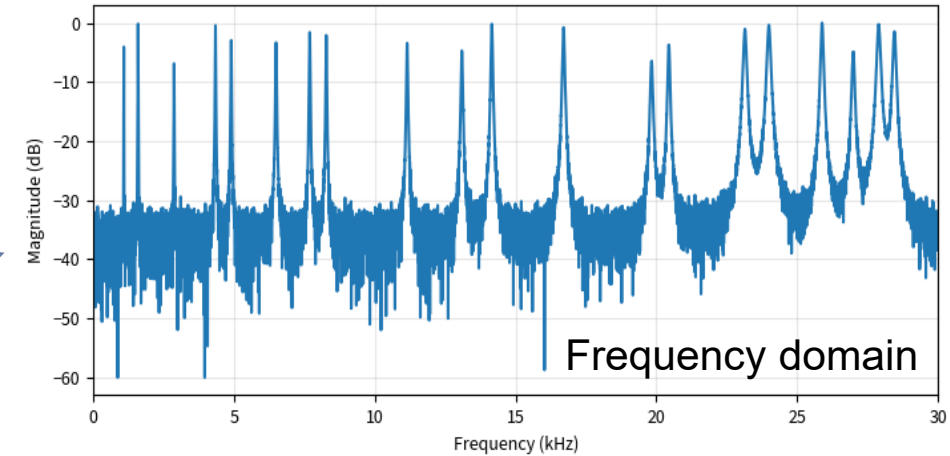


Accuracy: 93.1%

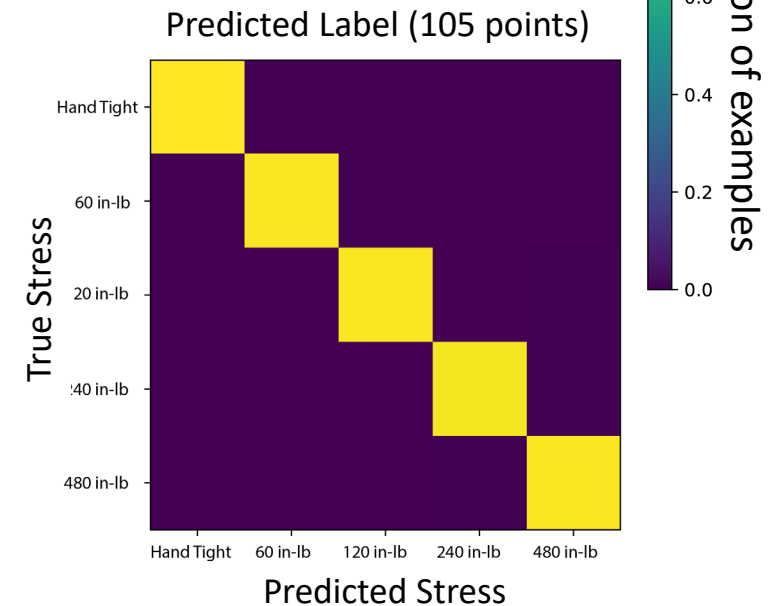
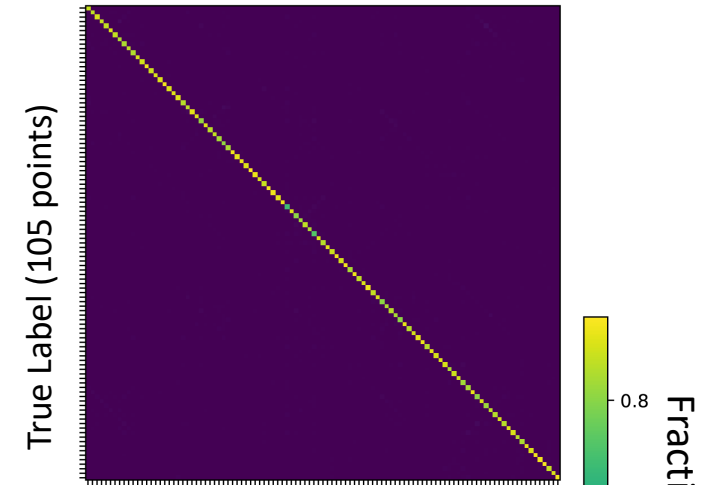
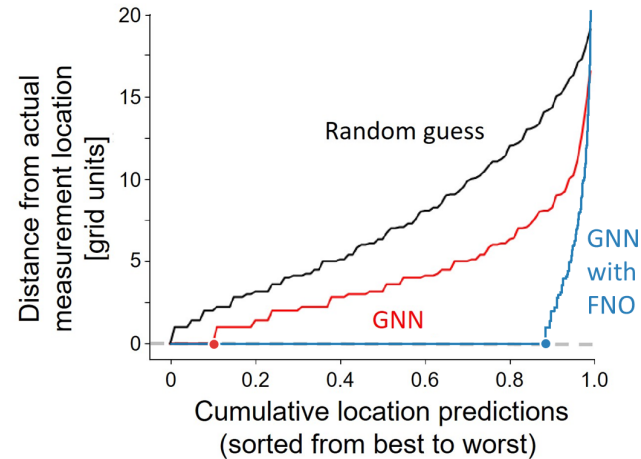
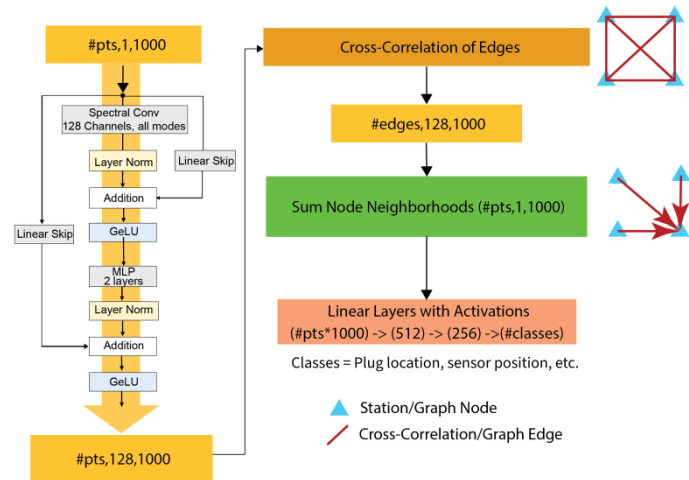
Actual label	Escaped particle	33	1	1
	Surface crack	2	21	0
	Shell non-uniformity	2	0	27
		Escaped particle	Surface crack	Shell non-uniformity
		Predicted label		

vs. accuracy of only ~80% when using traditional ultrasonic parameters

Pyun et al. (2025). Comprehensive defect evaluation of advanced nuclear fuels using high-resolution acoustic signals and optimized sensor separation
Nondestruct. Test. & Eval. Int.



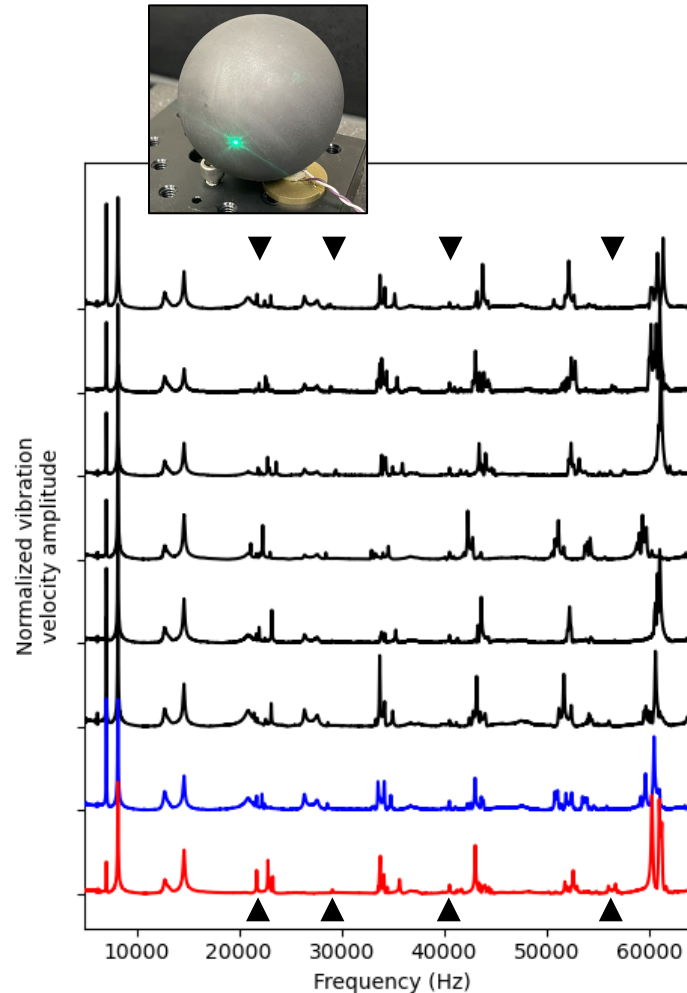
Machine learning implementation



- Graph Neural Network (GNN) enables arbitrary sensor placement
- Added Fourier Neural Operator (FNO) in FY25 to better capture spectral elastic behavior
 - Neural operators learn function-to-function mappings and generalizes well across grid sizes
- Compared to previous results, greatly improved localization and characterization through coupled workflow

Global inspection: Discrimination of sphere population using spectral features

- Prediction accuracy >99% due to small spectral differences caused by density and geometry variation
- High accuracy despite low-frequency (< 20 kHz) spectral contamination
- Material properties confirmed within spec.



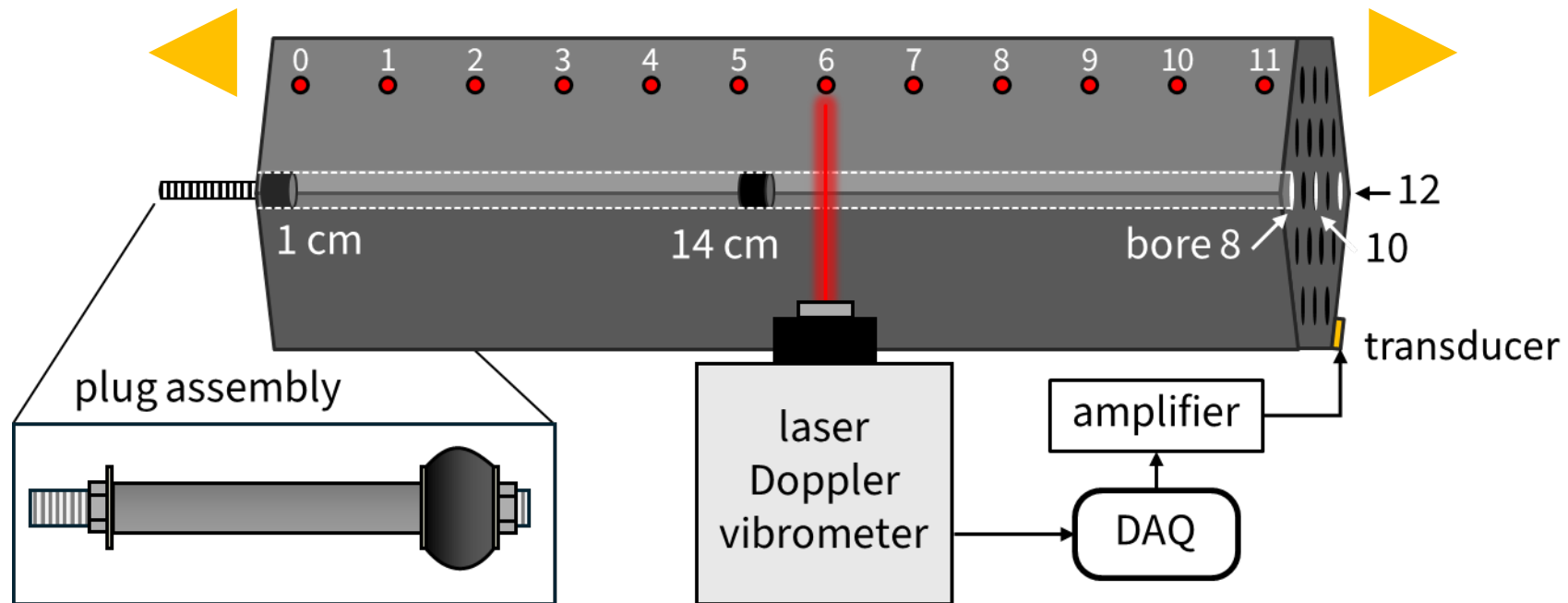
	Forward Model $E=11.5 \text{ GPa}, \nu=0.17$	Sphere A	Sphere B
Mode 1 [kHz]	 22.092	 21.986 (-0.5%)	 21.409 (-3.1%)
Mode 1 (degenerate) [kHz]	 22.093	 22.819 (+3.3%)	 21.721 (-1.7%)
Mode 3 [kHz]	 28.640	 29.005 (+1.3%)	 28.564 (-0.3%)
Mode 7 [kHz]	 40.869	 41.683 (+2.0%)	 41.102 (+0.6%)
Mode 13 [kHz]	 55.111	 56.015 (+1.6%)	 54.596 (-0.9%)

High
Low
Modal Displacement

Localized anomaly

Experimental setup 1:

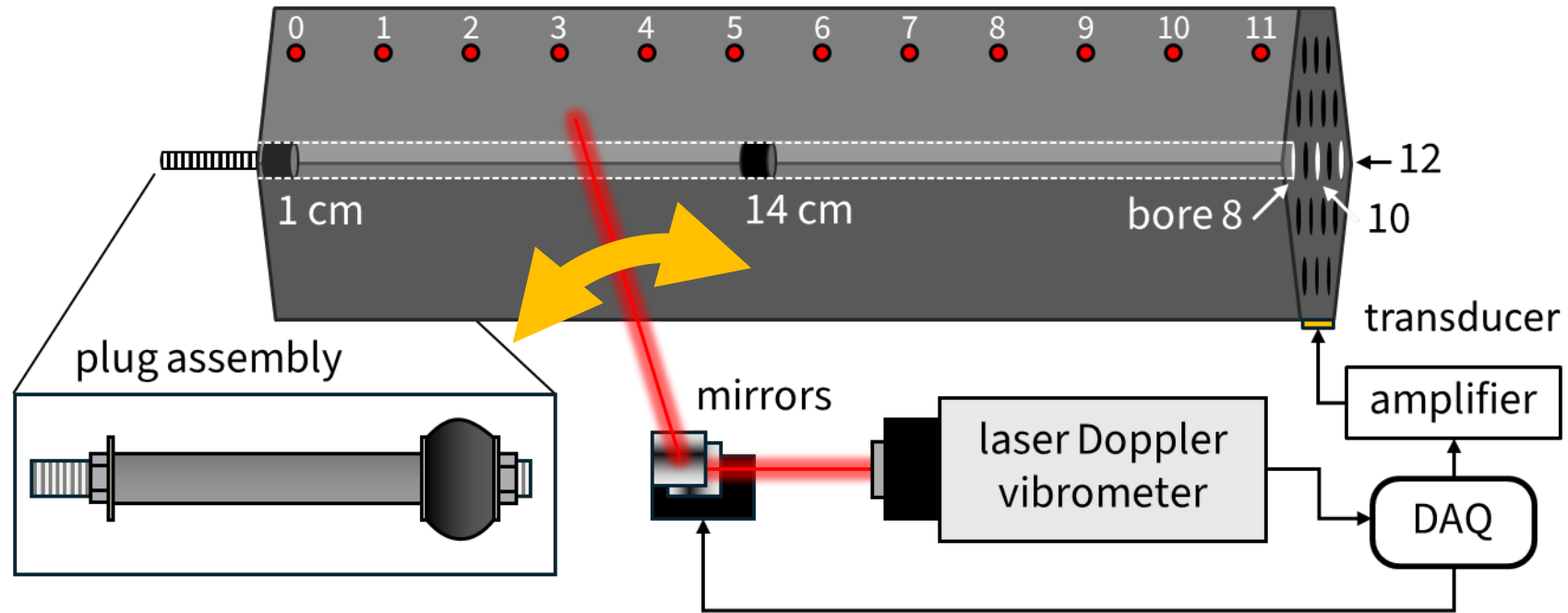
Stationary vibrometer, moving sample



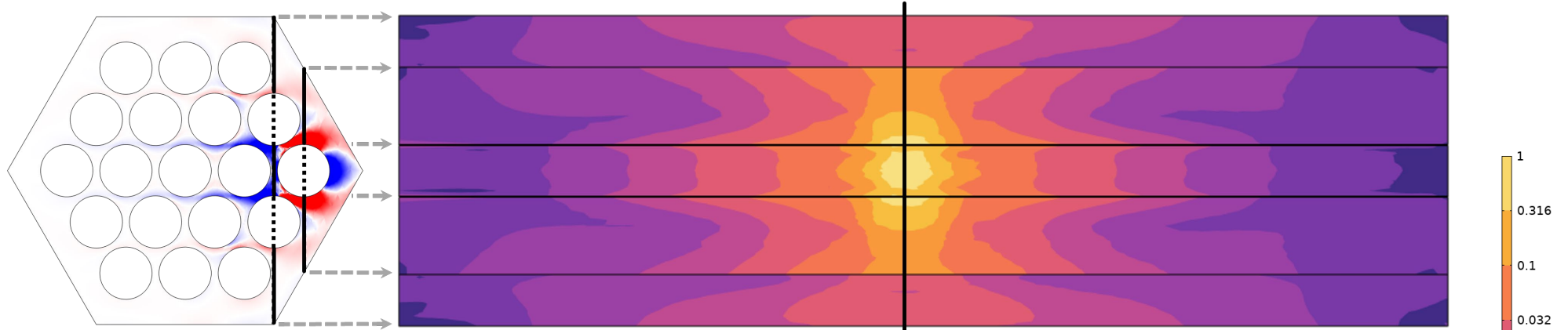
Localized anomaly

Experimental setup 2:

Scanning laser vibrometry, stationary sample

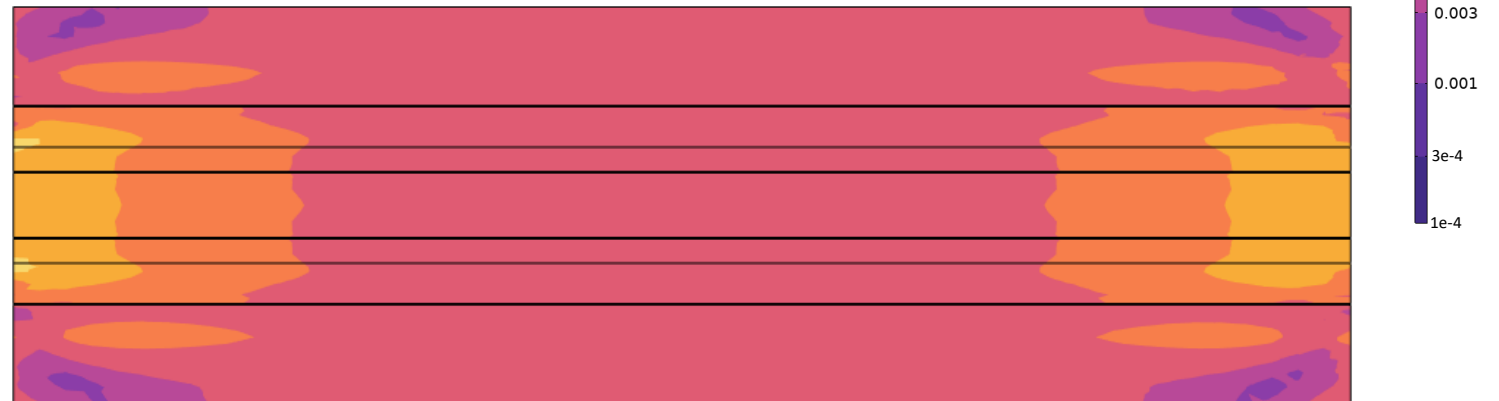


Local vs. uniaxial distribution of applied stress anomaly



Current: localized compression in graphite

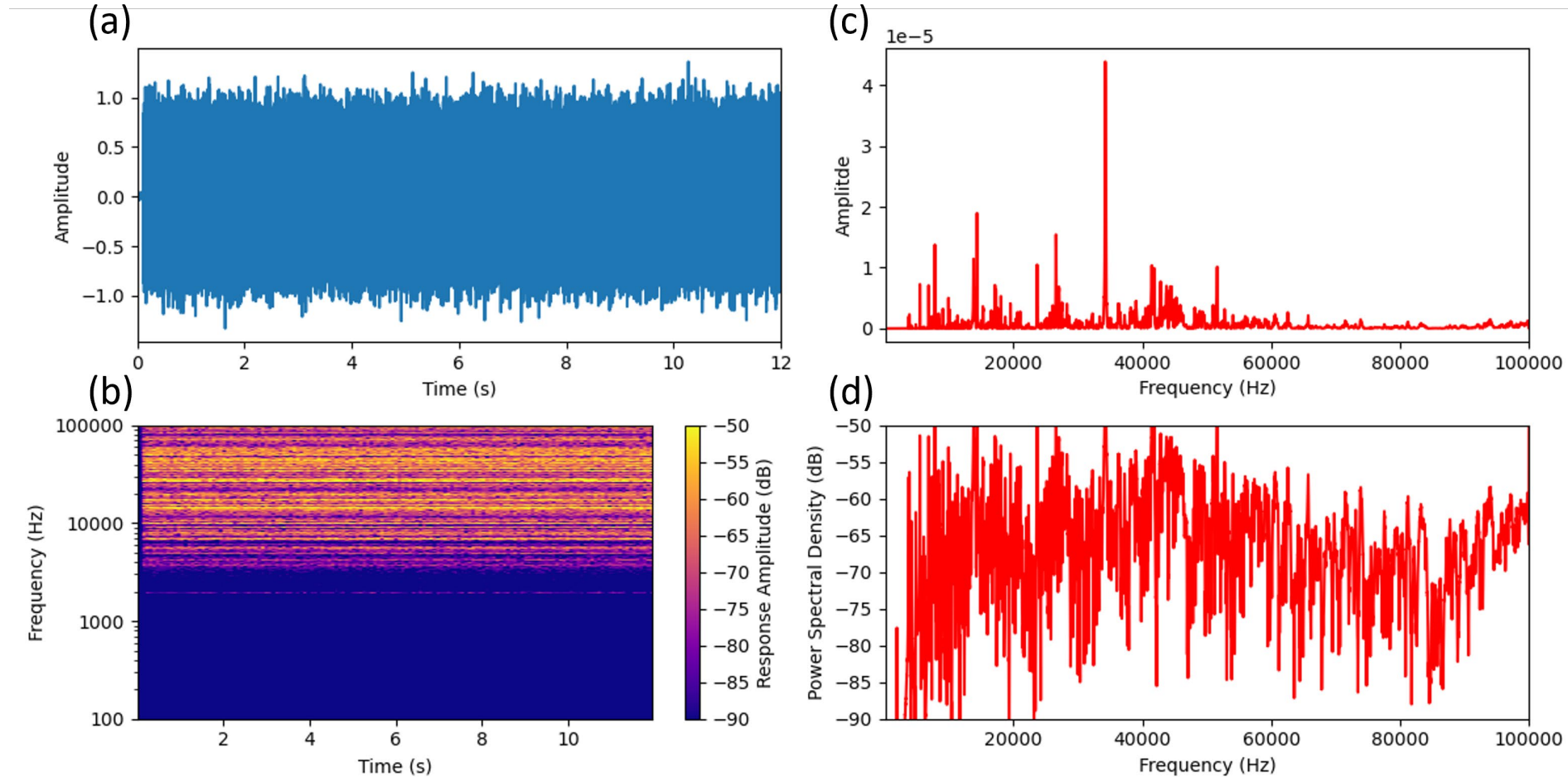
- Larger volume fraction impacted by uniaxial loading (bottom) as compared to localized load
 - Produces spatially complex pattern of **compressive** and **tensile** stresses



Previously: uniaxial compression in steel

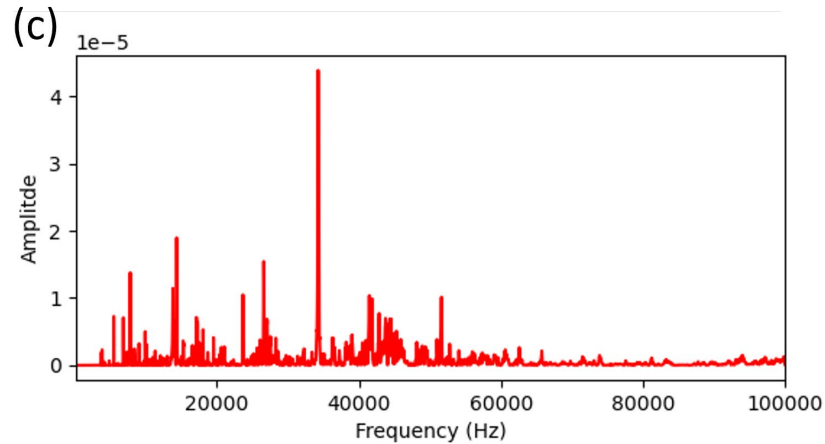
Preliminary data collection and processing (Approach 1)

- a) Time series
- b) Spectrogram
- c) Linear spectrum
- d) Power spectrum

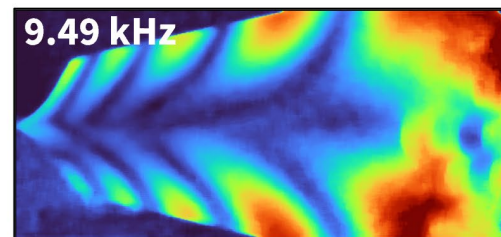
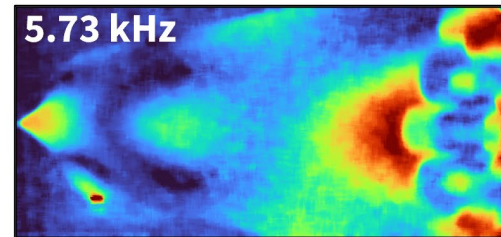
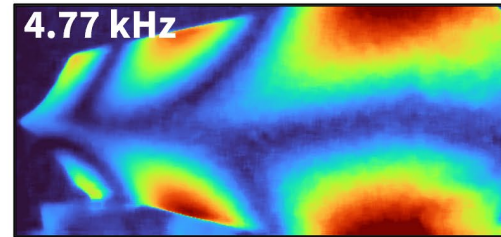


Validation of spectral features using modal analysis

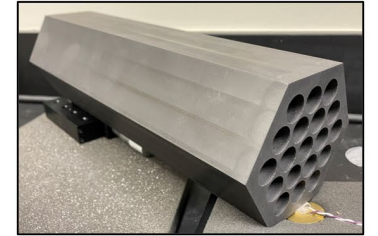
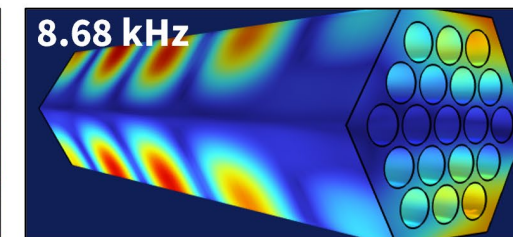
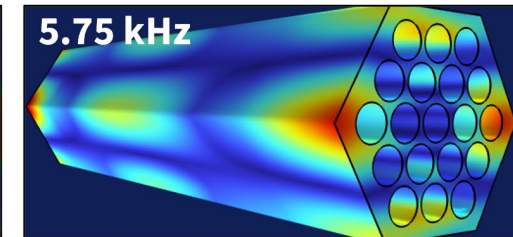
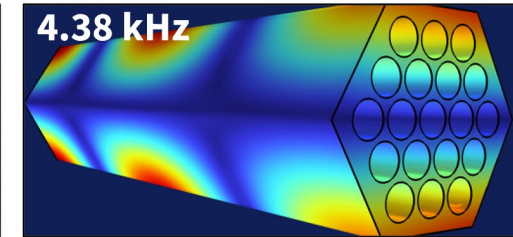
- Measured mode shapes correspond to identified peaks (sub-10 kHz shown)



Measured



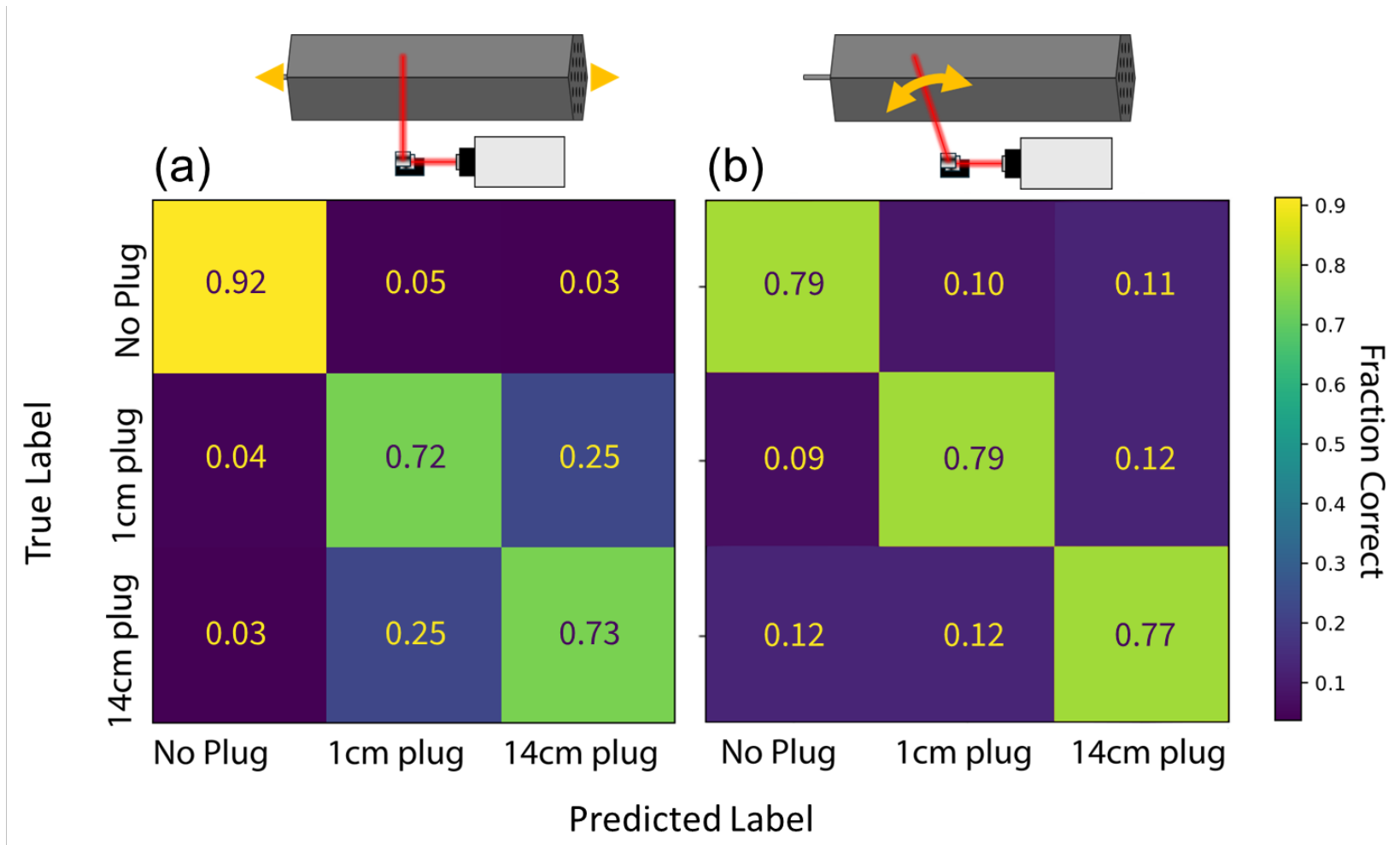
Modeled



Large
Line-of-sight
Displacement
Small

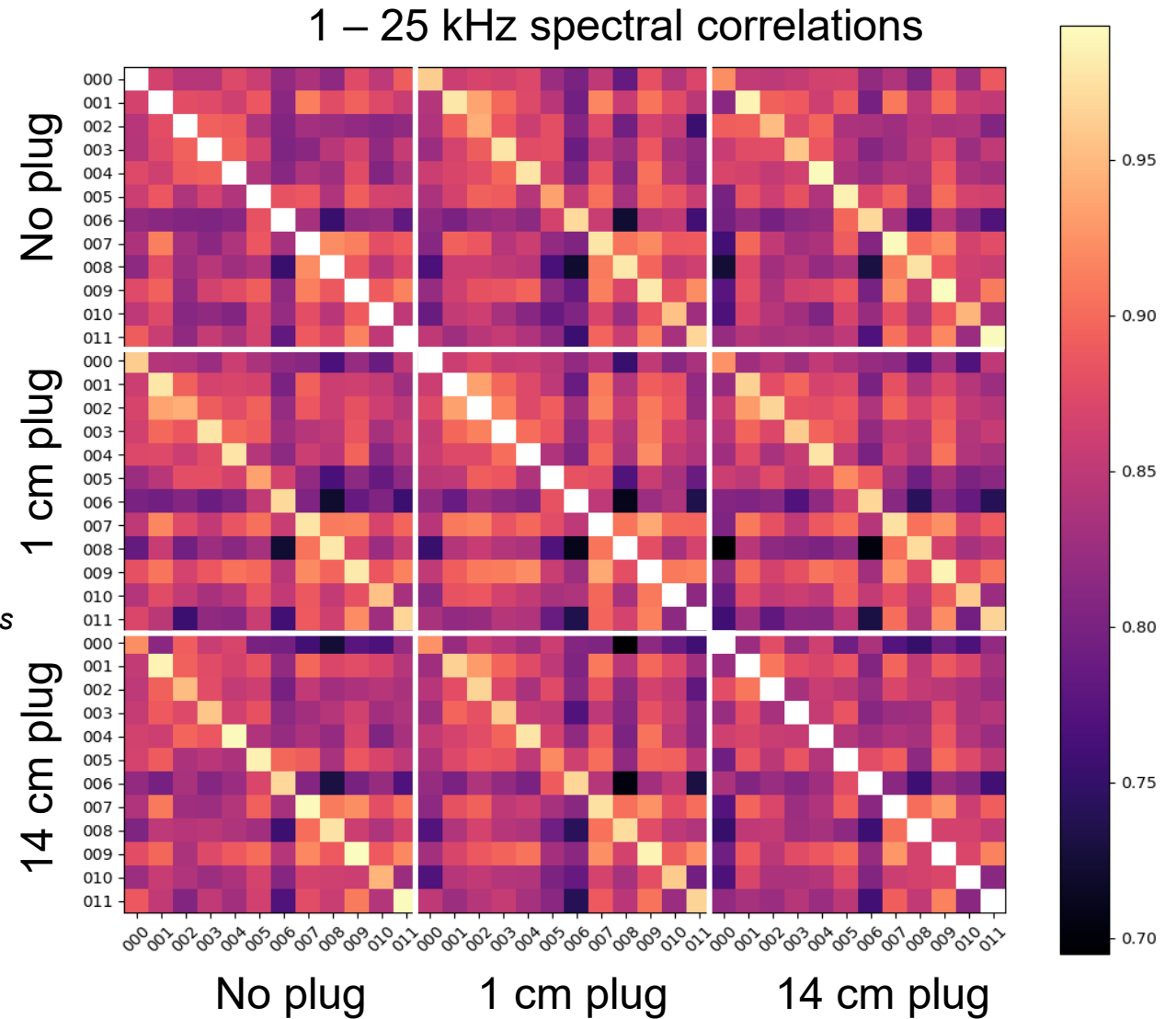
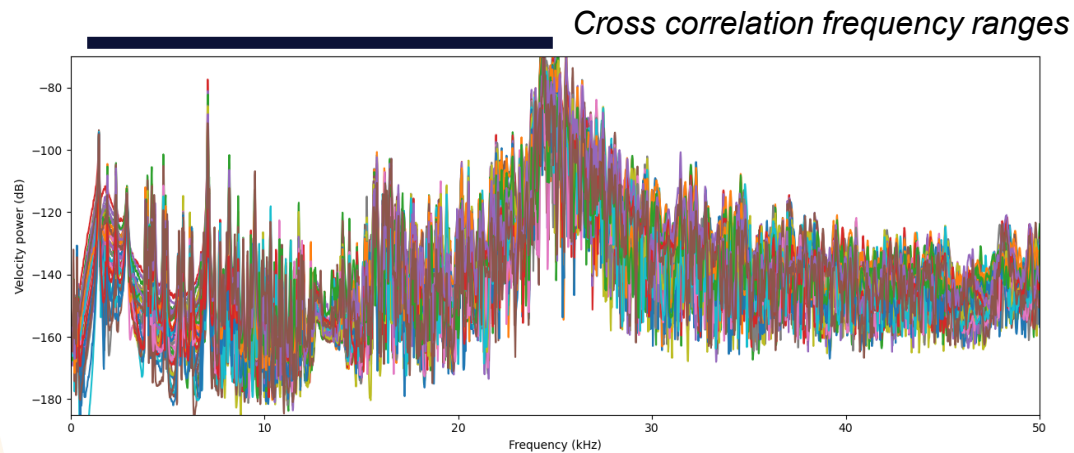
1D localization of blind anomaly

- Comparable accuracy for both testing approaches (off-axis values)
- Approach 2 preferred due to higher testing repeatability



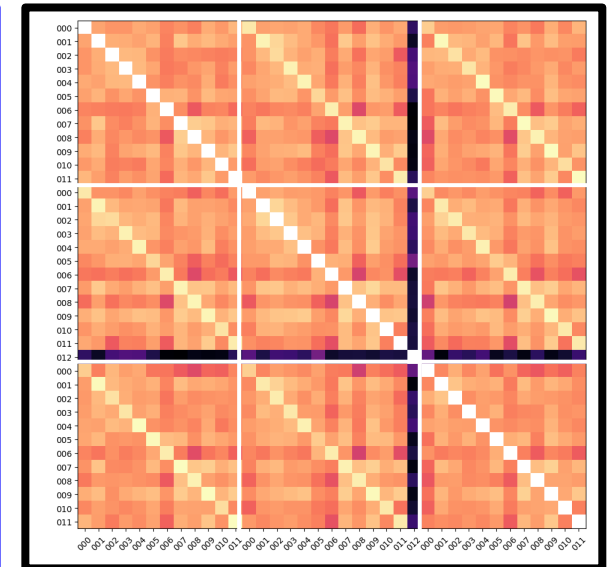
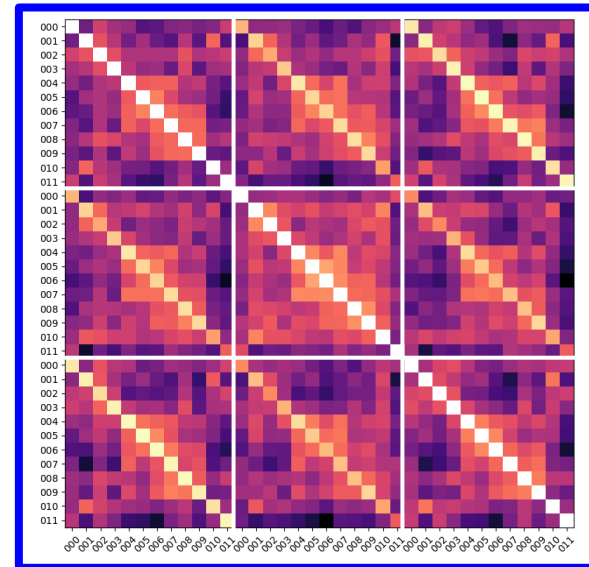
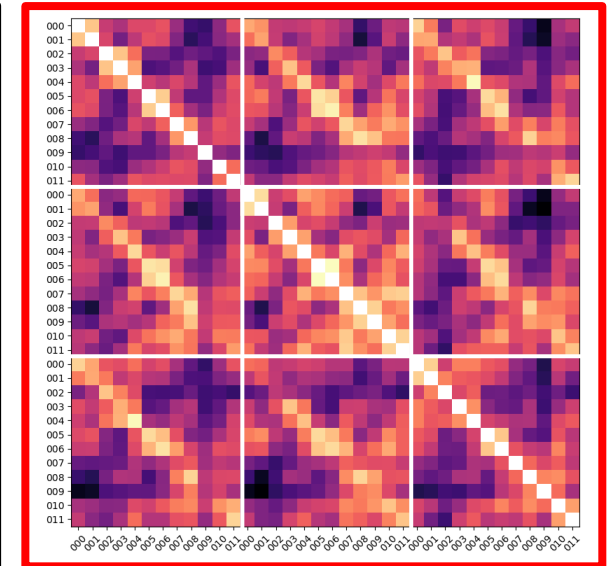
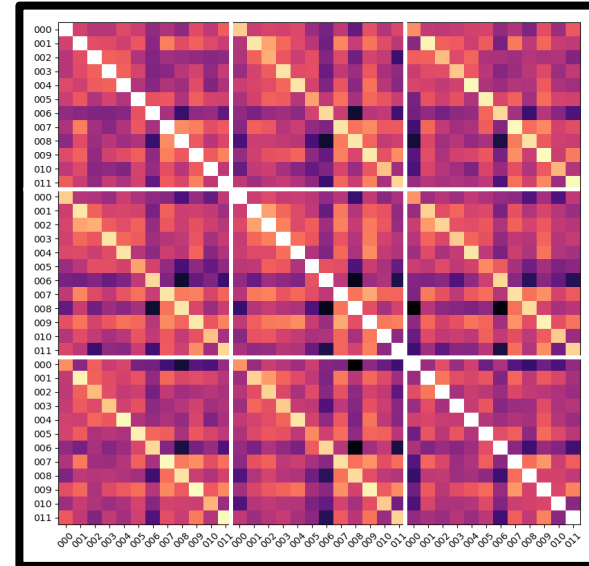
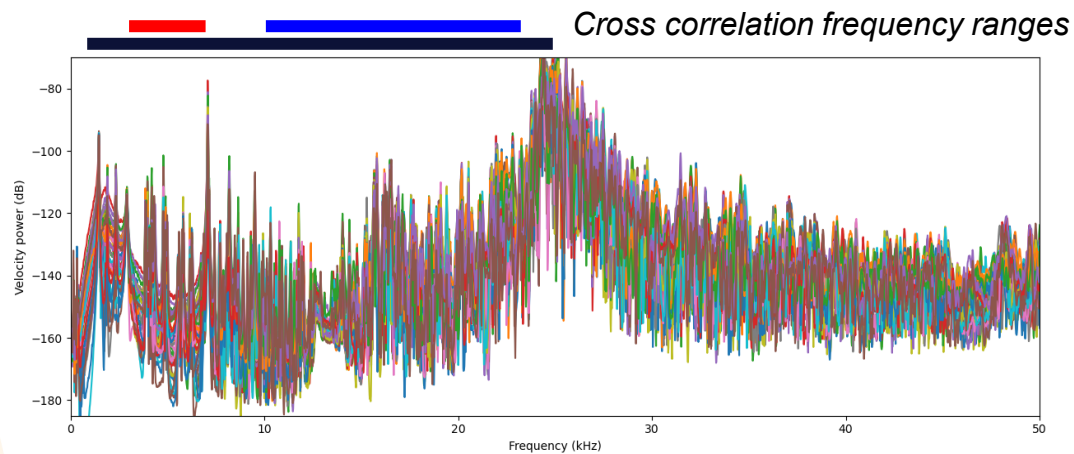
Cross correlations provide insights into model's learned features

- Strong location similarity (main and secondary diagonals)

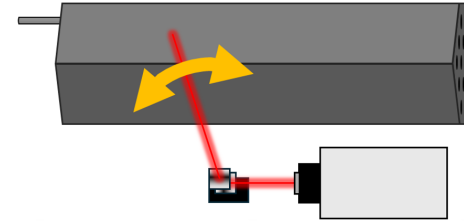


Cross correlations provide insights into model's learned features

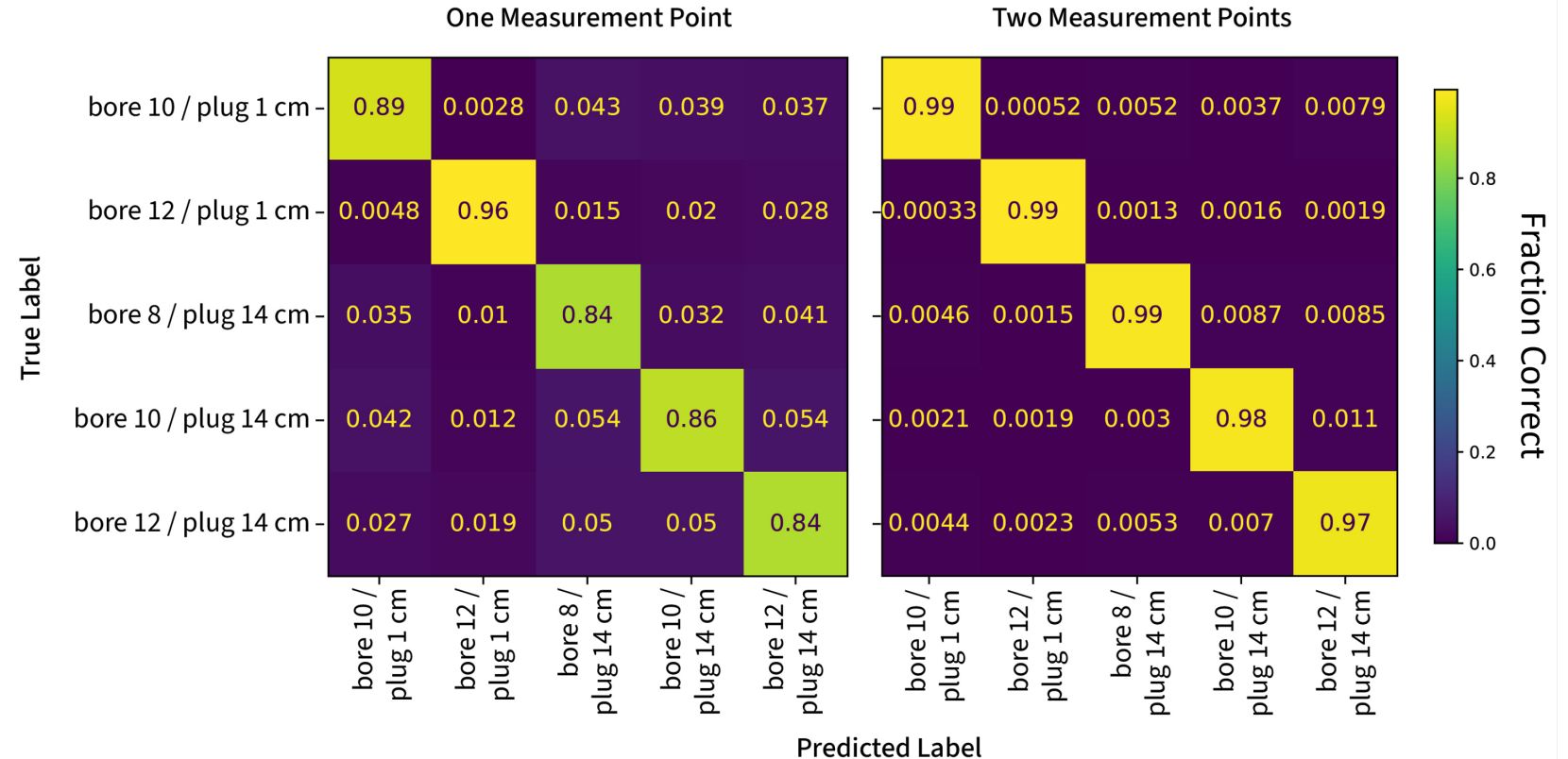
- Strong location similarity (main and secondary diagonals)
- Easily detects non-component spectral information (bottom right)



2D and pseudo-3D localization of blind anomaly



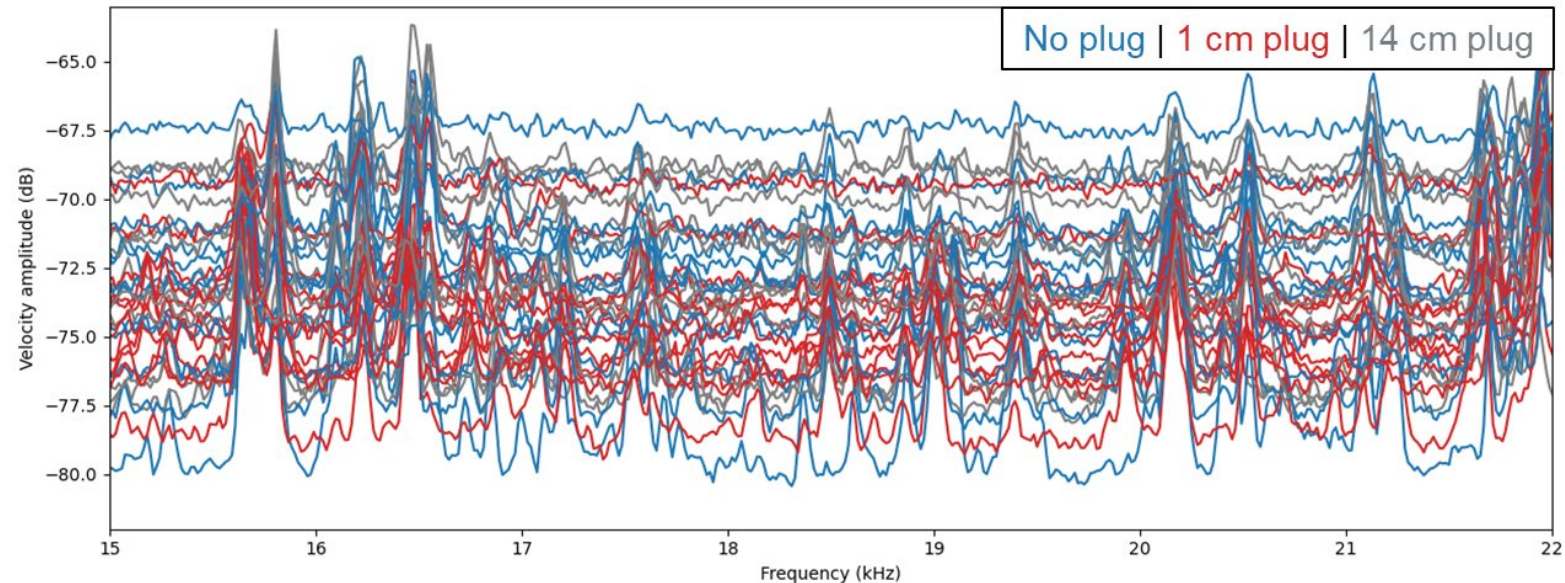
- Approach performs well using a single-station graphs
- Error reduced from ~12% to ~1.5% when second measurement point added to graph
- Approach is scalable for larger sensor graphs (e.g. distributed acoustic sensing, optical fibers, etc.)



Typical training times of ~1-10 hours
1 epoch took < 10 minutes

Impact of fluctuating noise levels within training data

- Baseline noise differences may bias model towards improved predictions
 - But median noise level was nearly identical (± 1 dB) across plug configurations, so this explanation is insufficient
- Addressed in most recent rounds of testing via bonded transducer and recalibrated laser



Opportunities for technique maturation

- Improve and streamline model to enable clear, floating-point predictions of unseen conditions
 - Ex. arbitrary anomaly locations (“12.2 cm”)
 - Focus for remainder of FY26
- Expand to larger variety of sensor types
 - Optical fibers (distributed acoustic sensing, fiber Bragg gratings, etc.)
- Test model against greater variety of damage scenarios and noise levels (steel vs. rubber insert)
- FNO implementation now published as Python module by paper authors (NeuralOperator), removing implementation barriers

bore 10 / plug 1 cm	0.89	0.0028	0.043	0.039	0.037
bore 12 / plug 1 cm	0.0048	0.96	0.015	0.02	0.028
bore 8 / plug 14 cm	0.035	0.01	0.84	0.032	0.041
bore 10 / plug 14 cm	0.042	0.012	0.054	0.86	0.054
bore 12 / plug 14 cm	0.027	0.019	0.05	0.05	0.84
bore 10 / plug 1 cm					
bore 12 / plug 1 cm					
bore 8 / plug 14 cm					
bore 10 / plug 14 cm					
bore 12 / plug 14 cm					



“A structural change has occurred in Zone 4 (87% probability)”

Summary

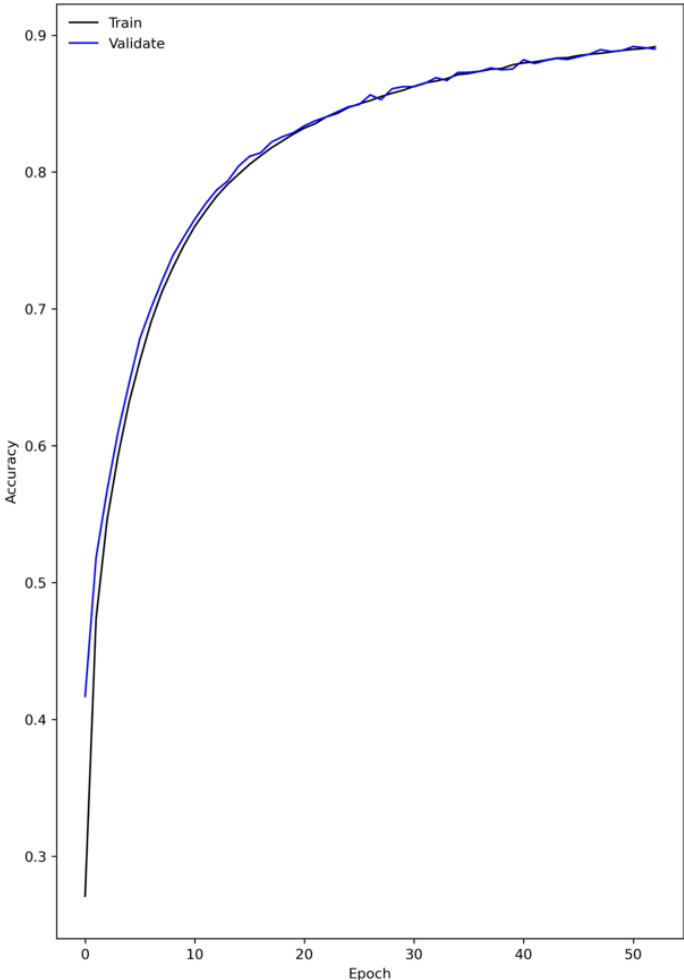
- Measured elastic-acoustic properties of graphite components using principles of modal analysis and machine learning
- Trained model predicted blind internal anomaly within graphite hex block
 - Encouraging performance in both 1D and 2D situations
 - Expansion of ML graph approach provides robust improvement in prediction accuracy

Recent Project Documentation

- M3 report from January 2026: “Graphite structural assessment through acoustic resonance and machine learning”
- End of FY25 report: “Non-destructive structural characterization of graphite components using mechanical resonance and deep learning”
- Manuscript in preparation for *Nondestructive Testing & Evaluation International*

Typical training and validation of FNO-GNN model

A: Sensor Location



B: Stress condition

